DOI:10.1158/0008-5472.CAN-06-1621

Cancer Research

# N-*myc* Is an Essential Downstream Effector of Shh Signaling during both Normal and Neoplastic Cerebellar Growth

Beryl A. Hatton, Paul S. Knoepfler, Anna Marie Kenney, et al.

*Cancer Res* 2006;66:8655-8661. Published online September 1, 2006.

DOI:10.1158/0008-5472.CAN-06-1621



# N-*myc* Is an Essential Downstream Effector of Shh Signaling during both Normal and Neoplastic Cerebellar Growth

**Beryl A. Hatton,[1,3] Paul S. Knoepfler,[2] Anna Marie Kenney,[5] David H. Rowitch,[6] Ignacio Moreno de Alborán,[7] James M. Olson,[1,4] and Robert N. Eisenman[2]**

[1]Clinical Research Division and [2]Division of Basic Sciences, Fred Hutchinson Cancer Research Center; [3]Graduate Program in Molecular and Cellular Biology, University of Washington; [4]Division of Pediatric Oncology, University of Washington/Children's Hospital, Seattle, Washington; [5]Cancer Biology and Genetics, Memorial Sloan-Kettering Cancer Center, New York, New York; [6]Department of Pediatric Oncology, Dana-Farber Cancer Institute and Harvard Medical School, Boston, Massachusetts; and [7]Department of Immunology and Oncology, National Center for Biotechnology, Madrid, Spain

## Abstract

**We examined the genetic requirements for the Myc family of oncogenes in normal Sonic hedgehog (Shh)–mediated cerebellar granule neuronal precursor (GNP) expansion and in Shh pathway–induced medulloblastoma formation. In GNP-enriched cultures derived from N-*myc*$^{Fl/Fl}$ and c-*myc*$^{Fl/Fl}$ mice, disruption of N-*myc*, but not c-*myc*, inhibited the proliferative response to Shh. Conditional deletion of c-*myc* revealed that, although it is necessary for the general regulation of brain growth, it is less important for cerebellar development and GNP expansion than N-*myc*. *In vivo* analysis of compound mutants carrying the conditional N-*myc* null and the activated *Smoothened* (ND2:SmoA1) alleles showed, that although granule cells expressing the ND2:SmoA1 transgene are present in the N-*myc* null cerebellum, no hyperproliferation or tumor formation was detected. Taken together, these findings provide *in vivo* evidence that N-*myc* acts downstream of Shh/Smo signaling during GNP proliferation and that N-*myc* is required for medulloblastoma genesis even in the presence of constitutively active signaling from the Shh pathway.** (Cancer Res 2006; 66(17): 8655-61)

## Introduction

Medulloblastoma is the most common childhood malignancy of the central nervous system and, despite aggressive multimodal therapy with surgery, radiation, and chemotherapy, 5-year survival rates have only approached recently >60% (1). Medulloblastomas are thought to derive from granule precursor cells of the cerebellum and comprise several histologic and prognostic subgroups. The desmosplastic subtype is distinguished from "classic" medulloblastoma by the presence of relatively acellular nodules within the dense sheets of malignant cells (2).

The mitogenic activity of the Sonic hedgehog (Shh) pathway is well characterized in the development of the cerebellum, where Shh drives the proliferation of granule neuronal precursors (GNP) in the external granular layer (EGL; refs. 3, 4). GNPs originate from the rhombic lip during embryonic development and then migrate out to cover the outer surface of the developing cerebellum during both late embryogenesis and the postnatal period, where they undergo significant expansion to form the EGL (5). Shh is secreted from Purkinje cells and binds to the Patched (PTCH) receptor on the GNPs, which relieves inhibition of the G-coupled transmembrane receptor Smoothened (Smo). Smo then activates the Gli family of zinc finger transcription factors (6–8) and the proto-oncogene N-*myc* (9), as well as expression of *cyclin D* and *cyclin E* (10), which together are thought to promote the proliferation of GNPs in the EGL (11).

Numerous studies have shown that deregulated Shh signaling is critical to the genesis and survival of both classic and desmoplastic subtypes of sporadic medulloblastoma (12–16). Genetic alterations associated with medulloblastoma include activating mutations in *Smo* and inactivating mutations in negative regulators of Shh signaling, such as *Ptch1* and *suppressor of fused* (*SUFU*). Thus, Shh signaling regulates normal cerebellar development, and deregulation of this signaling plays a critical role in the formation of medulloblastomas.

In addition to mutations in the *Ptch1, SUFU*, and *Smo* genes, amplifications of the proto-oncogenes N-*myc* and c-*myc* have also been observed in 5% to 8% of medulloblastoma cases (17). The Myc family of basic helix-loop-helix leucine zipper proteins act as transcriptional regulators that direct cell growth and proliferation, and Myc family members play a key role in promoting the progression of the cell cycle in proliferating cells (for reviews, see refs. 18, 19). *In vitro* studies with cultures enriched for GNPs have shown that treatment with soluble Shh protein up-regulates N-*myc* expression and that N-*myc* overexpression can promote GNP proliferation even in the absence of Shh treatment (9). Overexpression of c-*myc* in cultures of nestin-positive neural progenitors promoted their proliferation (20), but treatment of GNP-enriched cultures with Shh did not induce c-*myc* expression (9), suggesting that c-*myc* may not be transcriptionally regulated by Shh. Furthermore, expression of dominant-negative mutants of *myc* block the proliferative response induced by Shh (9, 21), and conditional knockout of N-*myc* within the brain severely disrupts the expansion of GNPs within the cerebellum (11), linking N-*myc* to normal granule cell development.

We reported previously a transgenic mouse model, in which the expression of a constitutively activated form of *Smoothened* (SmoA1) was driven in cerebellar GNPs through the use of the 1-kb *neuroD2* promoter (ND2:SmoA1; ref. 16), whose expression begins during embryonic development. The SmoA1 mutation was originally identified in cases of sporadic basal cell carcinoma, and the mutated Smo protein was shown to transform rat embryonic fibroblast cells in culture (22). Mutations that activate *Smo* have also been associated with sporadic brain tumors (23–25). The ND2:SmoA1 mice exhibit a high penetrance (48%) of cerebellar

**Note:** B.A. Hatton and P.S. Knoepfler contributed equally to this work.
R.N. Eisenman is an American Cancer Society Research Professor.

**Requests for reprints:** Beryl A. Hatton, Graduate Program in Molecular and Cell Biology, University of Washington/Fred Hutchinson Cancer Research Center, 1100 Fairview Avenue North, Mailstop D4-100, P. O. Box 19024, Seattle, WA 98109. E-mail: berylh@u.washington.edu.



doi:10.1158/0008-5472.CAN-06-1621

DOI:10.1158/0008-5472.CAN-06-1621



tumors that histologically resemble human medulloblastoma with a median tumor onset of 6 months (16).

Whereas the role of Shh in driving GNPs expansion within the developing cerebellum and the link between deregulated Shh signaling and medulloblastoma formation have been clearly established, the requirement for Myc family function has not been as well defined in Shh-induced tumorigenesis. In particular, previous studies have not examined the role of N-*myc* by genetic loss-of-function analysis in the context of medulloblastoma tumorigenesis. Furthermore, potential roles for the other major *myc* family member, c-*myc*, in GNP expansion are unknown. To address these important questions, we ablated N-*myc* or c-*myc* using Cre/lox conditional targeting both *in vitro* with cultured GNPs and *in vivo* with conditional knockout mice.

## Materials and Methods

**Cerebellar GNP cultures.** GNPs were isolated from wild-type (WT) N-*myc*$^{Fl/Fl}$ and c-*myc*$^{Fl/Fl}$ mice at postnatal day 5 (P5) and cultured overnight in the presence of Shh (3 μg/mL) and serum and then with Shh and without serum for 3 to 5 days as described previously (11, 26). For infection, Shh-conditioned medium was removed and cells were incubated with retroviral supernatants for 2 hours. Viral supernatants were then removed and Shh-conditioned medium was replaced. GNPs were infected on three sequential days leading to an infection rate of >90% as verified by green fluorescent protein (GFP) status. The biologically active, modified $NH_2$-terminal peptide of Shh was used for Shh-conditioned medium and provided by Curis, Inc. (Cambridge, MA).

**Retroviral constructs and virus production.** Amphotropic retrovirus was produced using the VSV-G system (27). Briefly, GFP or GFP-Cre retroviral MSCV plasmids were cotransfected with VSV-G helper plasmids into 293T cells. Two days later, conditioned medium containing virus was harvested and concentrated to 30× by centrifugation (Sorvall 20K G-30 minutes) and the viral pellet was then resuspended in GNP medium.

**Immunocytochemical labeling and analysis.** For analysis of proliferative capacity, GNP cultures were pulsed with 25 μg/mL bromodeoxyuridine (BrdUrd) for 2 hours before fixation in 4% paraformaldehyde. Cells were washed in PBS and treated with 2 N HCl. Fresh 2 N HCl was added again and cells were incubated for 30 minutes at room temperature. Cells were then immunocytochemically labeled using standard methods. Primary antibodies included mouse anti-BrdUrd and rabbit anti-N-*myc* (Santa Cruz Biotechnology, Santa Cruz, CA). Fluorochrome-conjugated secondary antibodies included tetramethyl rhodamine isothiocyanate–conjugated anti-mouse and anti-rabbit IgG (Jackson Immunoresearch Laboratories, West Grove, PA). A 4′,6-diamidino-2-phenylindole (DAPI) costain was used to label cell nuclei. Staining was visualized with a Zeiss Axioskop 40 microscope and images were captured with an Axiocam MRm digital camera. For all BrdUrd quantification studies, 100 to 200 cells from 3 independent fields were counted for each sample.

**Generation of conditional c-*myc* null mice.** Transgenic mice were maintained in accordance with the NIH Guide for the Care and Use of Experimental Animals with approval from our Institutional Animal Care and Use Committee (IR# 1064). c-*myc*$^{Fl/Fl}$ mice (28) were crossed to nestin-Cre mice (29) to create c-*myc*$^{Fl/WT}$ nestin-Cre mice. These heterozygous mice were then crossed to c-*myc*$^{Fl/Fl}$ mice to generate mice null for c-*myc* in neural stem and progenitor cells. The number of mice null for c-*myc* matched that predicted by Mendelian inheritance, showing that this combination was not embryonic lethal. Animals were generated on a mixed C57Bl/6 and 129 background.

**Generation of combined N-*myc* conditional knockout and ND2:SmoA1 mice.** Transgenic mice were maintained in accordance with the NIH Guide for the Care and Use of Experimental Animals with approval from our Institutional Animal Care and Use Committee (IR# 1457). A two-step breeding strategy was used to combine the two transgenic mouse models, which resulted in 12 different possible genotypes. These 12 genotypes were then further subdivided (see Table 1) for phenotypic and histologic analysis. Animals were generated on a mixed C57Bl/6 and 129 background.

**Mouse pathology.** Mice were euthanized using $CO_2$ inhalation; the brains were removed and tissue was fixed in 4% paraformaldehyde for pathologic examination. Tissue blocks were paraffin embedded, cut into 4-μm sections, and stained with H&E using standard methods. For examination of the four groups of mice from the combined N-*myc* conditional knockout and ND2:SmoA1 models, persistent EGL was defined as pockets of granule cells remaining in the molecular layer; hyperplasia was defined as morphologically abnormal populations of cerebellar granule cells; a tumor was defined as sheets of small round blue cells without identifiable cerebellar architecture. For analysis of ND2:SmoA1 expression, sections were processed with standard immunohistochemical methods. A monoclonal anti-PentaHis antibody (Molecular Probes, Eugene, OR) was used with a FITC-conjugated anti-mouse IgG antibody (Jackson Immunoresearch Laboratories) and a DAPI costain was used to label cell nuclei. For Ki-67 and nesting staining, a polyclonal Ki-67 antibody (Santa Cruz Biotechnology, Santa Cruz, CA) and a monoclonal nestin antibody (Chemicon International, Temecula, CA) were used; secondary antibodies applied according to Vectastain Elite avidin-biotin complex method instructions (Vector Laboratories, Burlingame, CA) and detection were carried out with 3,3′-diaminobenzidine reagent (Vector Laboratories). Cells were visualized with a Zeiss Axioscope 40 microscope and images were captured with a Qimaging MicroImager II digital camera.

## Results and Discussion

**N-*myc* is required for the proliferative response of cultured GNPs to Shh.** GNPs were isolated from N-*myc*$^{Fl/Fl}$ mice and WT control mice at the height of their postnatal expansion (P5), cultured as described previously (26), and infected with retroviruses encoding bicistronic Cre recombinase and GFP. A retrovirus expressing GFP alone was used as a control. GNPs were cultured in the presence of Shh (3 μg/mL) throughout the

**Table 1.** Histologic analysis of combined conditional N-*myc* knockout × ND2:SmoA1 mice

| Genotype | Time point, mo (*n*) | Tumor formation | Hyperplasia | Persistent EGL | Diminished cerebella | Reduced foliation |
|---|---|---|---|---|---|---|
| WT N-*myc*, SmoA1$^+$ | 3 (20) | 1 | 11 | 16 | 0 | 0 |
| | 6 (37) | 12 | 19 | 29 | 0 | 0 |
| WT N-*myc*, SmoA1$^-$ | 3 (3) | 0 | 0 | 0 | 0 | 0 |
| | 6 (7) | 0 | 0 | 0 | 0 | 0 |
| N-*myc* null, SmoA1$^+$ | 3 (12) | 0 | 0 | 0 | 12 | 12 |
| | 6 (9) | 0 | 0 | 0 | 9 | 9 |
| N-*myc* null, SmoA1$^-$ | 3 (5) | 0 | 0 | 0 | 5 | 5 |
| | 6 (2) | 0 | 0 | 0 | 2 | 2 |

DOI:10.1158/0008-5472.CAN-06-1621



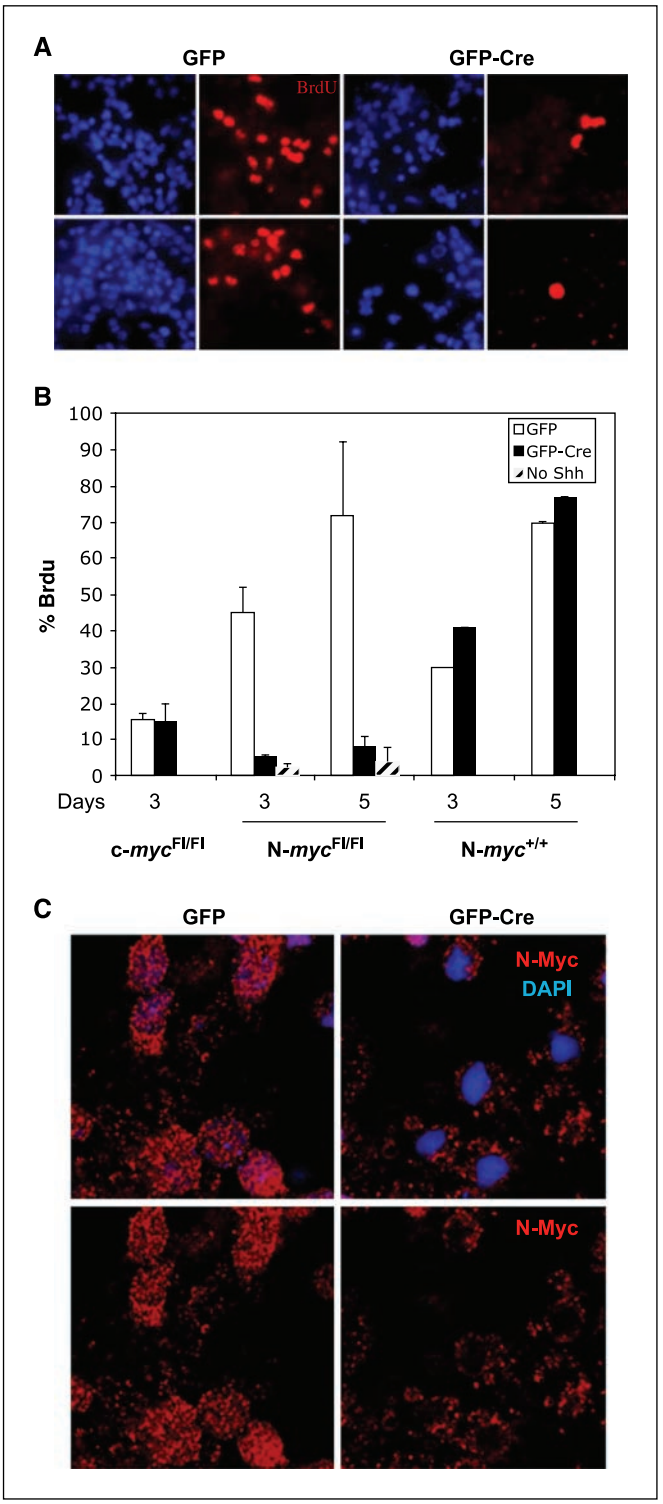


**Figure 1.** Acute knockout of N-*myc* strongly blocks progenitor proliferation in response to Shh. *A,* GNP cultures isolated from P5 N-*myc*$^{Fl/Fl}$ mice and WT control mice were infected with retroviruses encoding GFP-Cre recombinase or GFP alone as a control. GNPs were cultured in the presence of Shh and pulsed with BrdUrd 2 hours before fixation in 4% paraformaldehyde, stained with anti-BrdUrd (*red*) and costained with DAPI to label cell nuclei (*blue*), and examined using fluorescent microscopy. *B,* quantification of BrdUrd incorporation in GNPs isolated from c-*myc*$^{Fl/Fl}$, N-*myc*$^{Fl/Fl}$, and WT mice at 3 and 5 days after infection with GFP-Cre or the GFP control. *Bars,* SE. *C,* control GFP and GFP-Cre-infected GNP cultures were stained with fluorescent-tagged anti-N-*myc* (*red*) and DAPI (*blue*) to verify N-*myc* deficiency induced by the Cre recombinase.

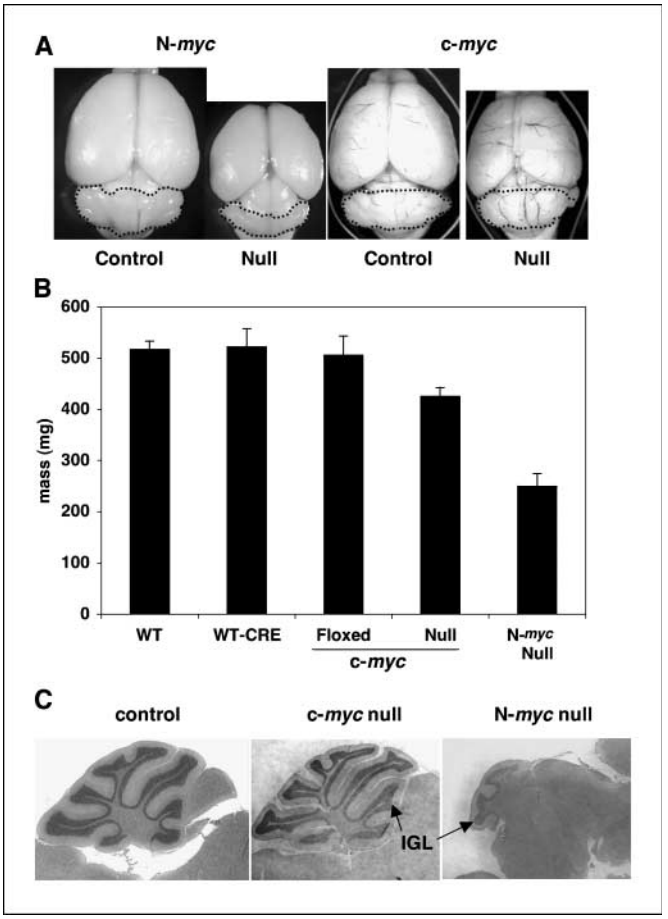


**Figure 2.** Loss of c-*myc* does not disrupt cerebellar development *in vivo* but retards overall brain growth. *A,* c-*myc*$^{Fl/WT}$ nestin-Cre mice were crossed to c-*myc*$^{Fl/Fl}$ mice to generate mice null for c-*myc*. The conditional N-*myc* knockout mice were generated as described previously (11). Whole brains from 2- to 3-month-old mice are shown with their cerebella outlined. Note that, although the overall size of the c-*myc* null brain is moderately decreased compared with the control brains lacking nestin-Cre expression, the development of the c-*myc* null cerebellum was not specifically impaired in contrast to the conditional N-*myc* knockout mouse brain. *B,* mice lacking c-*myc* displayed an 18% reduction in total brain mass compared with WT, WT Cre-positive, and c-*myc*$^{Fl/Fl}$ Cre-negative controls. The data on N-*myc* null brain mass were reported previously (11). *Bars,* SE. *C,* sagittal sections of mouse cerebella from control, c-*myc* null, and N-*myc* null mice at 2 to 3 months of age were stained with H&E after fixation in 4% paraformaldehyde.

experiment. At 5 days after infection, GFP-Cre-infected cells were verified to be N-*myc* deficient by immunofluorescent staining (Fig. 1*C*). We have found previously that such N-*myc* null GNPs display no change in apoptosis or in specification of granule cell identity as determined by cleaved caspase-3 and Zic1 immunofluorescence, respectively (30). At 3 and 5 days following infection, control and null GNPs were pulsed for 2 hours with BrdUrd to label $G_1$ and S phase cells and then fixed and stained to examine BrdUrd incorporation. In both WT and GFP-infected control cultures by day 5, ~80% of cells incorporated BrdUrd, indicating a highly proliferative population. In contrast, only 10% of the N-*myc*-deficient cells incorporated BrdUrd, an 8-fold reduction (Fig. 1*A* and *B*). A similar level of reduced proliferation is observed in knockout GNPs derived from N-*myc*$^{Fl/Fl}$ nestin-Cre P5 pups.[8]

[8] P.S. Knoepfler and Robert N. Eisenman, unpublished data.

DOI:10.1158/0008-5472.CAN-06-1621



The markedly reduced levels of proliferation in N-*myc* null cells were similar to those seen in GNPs cultured in the absence of Shh (Fig. 1*B*), suggesting that N-*myc* is an essential downstream effector of Shh signaling.

**c-*myc* function is generally required for normal brain growth but has no specific roles in cerebellar development.** N-*myc* is expressed in the proliferative region of the EGL, where Shh activity has been shown to drive GNP proliferation (4, 9, 31). These studies indicated that N-*myc* is the only *myc* family member in the cerebellum that is regulated by Shh and raised the possibility that N-*myc* may have a unique role in the proliferative expansion of GNPs, a notion supported by studies showing that the conditional knockout of N-*myc* within the developing nervous system prevented the full expansion of GNPs (11). Nonetheless, c-*myc* is also expressed in the developing brain (32) and low levels or transient expression of c-*myc* could potentially contribute to GNP growth.

To further address the role of c-*myc* in the development of the cerebellum, we conditionally knocked out c-*myc* in neural stem and progenitor cells *in vivo* using nestin-Cre. As shown in Fig. 2*A*, mice conditionally null for c-*myc* did not display a cerebellum-specific phenotype as was seen in the conditional N-*myc* knockout mice (11). Although the overall size of the c-*myc* null brain was diminished (18% reduction; Fig. 2*B*) compared with that of control mice, the expansion of GNPs and the development of the cerebellum were not specifically impaired by the loss of c-*myc* (Fig. 2*A*). The cerebella of animals lacking c-*myc* resembled those of control animals in the thickness of the inner granular layer (IGL) as well as in the extent of cerebellar foliation (Fig. 2*C*). In contrast, animals lacking N-*myc* in neural stem and progenitor cells displayed a reduction in total brain mass (Fig. 2*B*) and a failure in full expansion of the GNPs (Fig. 2*C*) as was shown previously (11).

To examine whether the acute loss of c-*myc* would have a similar effect on the proliferative response of GNPs to Shh *in vitro*, Cre/lox conditional targeting was used to knockout c-*myc* in primary GNP cultures. Cultures were infected with the GFP-Cre retrovirus or the control GFP virus, pulsed with BrdUrd 3 days after infection, and fixed and stained to examine BrdUrd incorporation. The infection of c-$myc^{Fl/Fl}$ GNP cultures with the GFP-Cre or GFP control retroviruses did not affect their proliferative response to Shh in either case. Approximately equal fractions of both control and GFP-Cre infected cells incorporated BrdUrd (Fig. 1*B*), indicating that c-*myc* is dispensable for the proliferative response of GNP cultures to Shh. The levels of BrdUrd incorporation were lower in the control c-$myc^{Fl/Fl}$ cultures infected with GFP alone compared with the control GFP-infected N-$myc^{Fl/Fl}$ or WT cultures due to experimental variability in the preparation of the cultures. Note that N-$myc^{Fl/Fl}$ cultures infected with GFP-Cre had incorporation levels below both c-$myc^{Fl/Fl}$ and WT cultures infected with either GFP-Cre or GFP alone. Thus, it seems that both c-*myc* and N-*myc* have important roles in the overall growth of the brain but that N-*myc* has a more critical role in cerebellar development and specifically in the expansion of GNPs. Because the function of N-*myc* was clearly critical to the proliferation of GNP cultures in response to Shh, we chose to examine the requirement for N-*myc* in the context of ND2:SmoA1-driven cerebellar hyperplasia and tumor formation.

**N-*myc* functions downstream of Smo and is necessary for the hyperproliferation induced by constitutive activation of the Shh pathway.** In addition to the formation of medulloblastomas, 55% of mice carrying the ND2:SmoA1 transgene display hyperproliferation of the granular layer by 3 months of age (Table 1). Expanded pockets of granule cells are present in the IGL of these mice, indicative of the excess proliferation of these cells. Furthermore, 80% of ND2:SmoA1 mice have a persistent EGL (Table 1), which is normally absent by postnatal day 20 in WT mice (17). These populations of cells also express the nuclear antigen Ki-67 (Fig. 3*A* and *B*), which marks proliferative cells, and the neural stem cell marker nestin (Fig. 3*E* and *F*), indicating that the presence of the

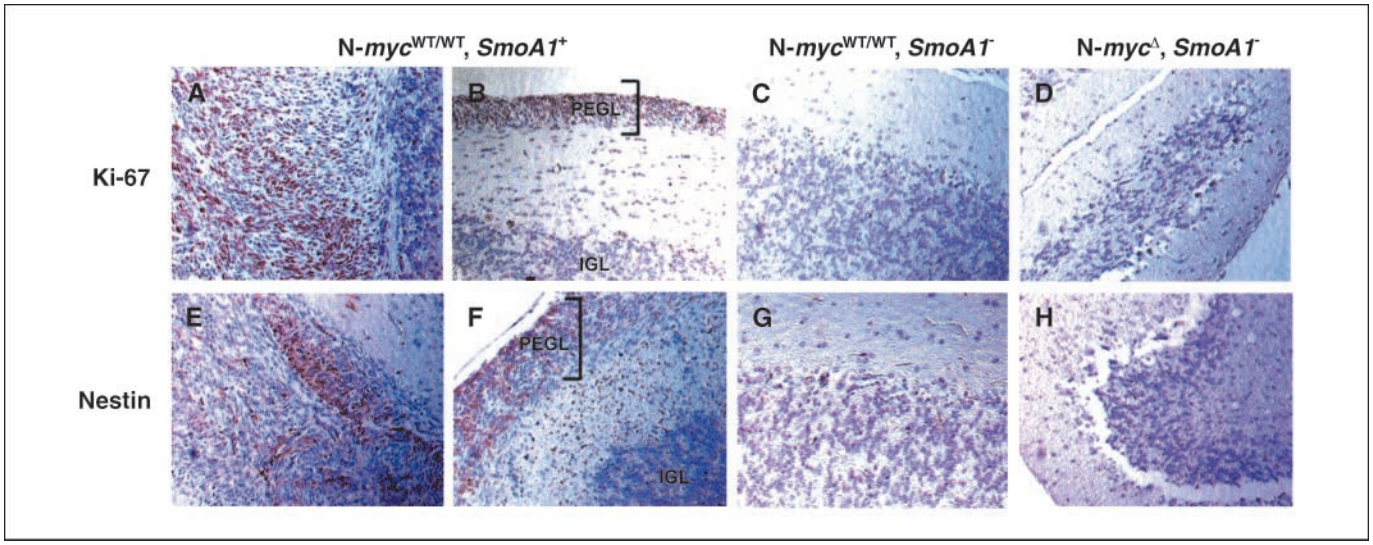


**Figure 3.** Regions of hyperplasia and persistent EGL (*PEGL*) express Ki-67 and nestin in N-$myc^{WT/WT}$, $SmoA1^+$ cerebella. Cerebellar sections from 3-month-old N-$myc^{WT/WT}$, $SmoA1^+$ mice displaying immunoreactivity for the mitotic marker Ki-67 (*A*) and the neural stem cell marker nestin (*E*) in regions of granule cell hyperplasia. Cerebellar sections from N-$myc^{WT/WT}$, $SmoA1^+$ mice displaying immunoreactivity for Ki-67 (*B*) and nestin (*F*) in regions with a persistent EGL, whereas cells in the IGL express neither marker. Immunohistochemical staining with antibodies against Ki-67 (*C*) and nestin (*G*) in cerebellar sections from 3-month-old WT mice (N-$myc^{WT/WT}$, $SmoA1^-$) shows that neither Ki-67 nor nestin is expressed. Similarly, no Ki-67 (*D*) or nestin (*H*) expression was observed in the cerebella of mice lacking N-*myc* and positive for the ND2:SmoA1 transgene (N-$myc^?$, $SmoA1^+$). *Brown,* positive staining; *light blue,* a nuclear haematoxylin counterstain. Magnification, ×40 magnification.

DOI:10.1158/0008-5472.CAN-06-1621



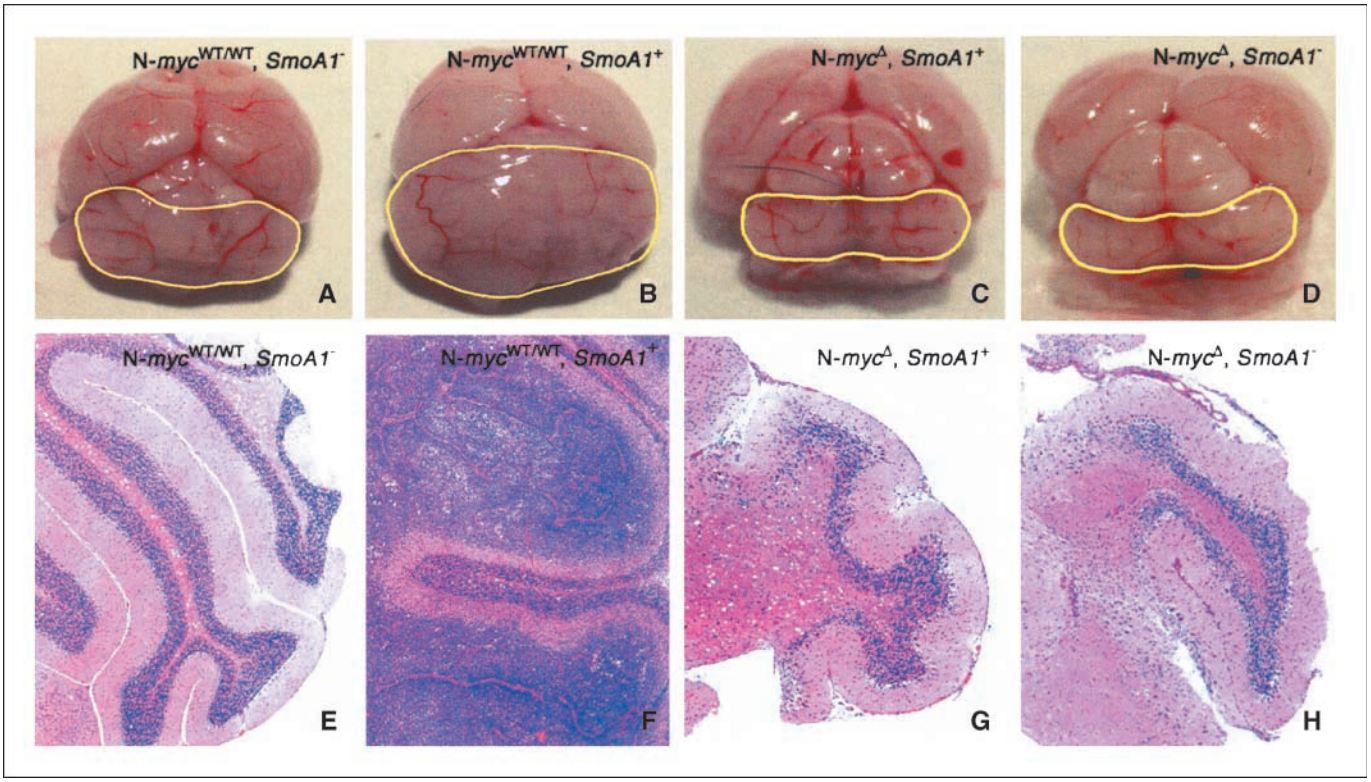


**Figure 4.** N-*myc* is essential for the hyperplasia and tumorigenesis induced by deregulated Shh signaling. *A* and *E,* representative brain and H&E-stained cerebellar section from an N-*myc*$^{WT/WT}$, SmoA1$^-$ mouse (WT control) at 6 months of age. *B* and *F,* example of a tumor in an N-*myc*$^{WT/WT}$, ND2:SmoA1$^+$ mouse. Sheets of small round blue cells disrupt the overall cerebellar architecture, with normal granule cell organization remaining only in small areas of the cerebellum (*F*). Representative brain and H&E-stained cerebellar section from an N-*myc*$^{\Delta}$, SmoA1$^+$ mouse (*C* and *G*) and from a mouse lacking both N-*myc* and the ND2:SmoA1 transgene (N-*myc*$^{\Delta}$, SmoA1$^-$; *D* and *H*). Mice lacking N-*myc* exhibit an overall reduction in size of cerebellum, diminished thickness of granule cell layer, and incomplete foliation in both the presence (*G*) and absence (*H*) of the ND2:SmoA1 transgene. Additionally, no hyperplasia, persistent EGL, or tumor formation is evident in N-*myc*$^{\Delta}$, SmoA1$^+$ mice (see Table 1). Whole brains in (*A-D*) were photographed at 6 months of age and the cerebella have been outlined in yellow; note that the relative differences in cerebellar size were also found in brains from 3-month-old mice. H&E-stained cerebellar sections taken at 6 months are shown at ×5 magnification in (*E-H*). Note that relative differences in cerebellar histology were also found in brains from 3-month-old mice.

ND2:SmoA1 transgene may sustain granule neural precursors in a progenitor state. Ki-67 and nestin expression was not seen in WT controls (Fig. 3*C* and *G*) or in ND2:SmoA1 cerebella lacking hyperplastic or persistent EGL phenotypes. This granule cell hyperplasia and the persistent EGL observed at 3 months may thus represent early stages in the formation of cerebellar tumors in the ND2:SmoA1 mice. Real-time PCR analysis showed that N-*myc* expression is elevated in cerebellar tumors generated in the ND2:SmoA1 medulloblastoma model (16), suggesting that the overexpression of N-*myc* may be involved in the initiation of hyperplasia and progression to tumor formation in SmoA1-induced medulloblastoma.

To determine whether N-*myc* is necessary for the hyperproliferation of GNPs seen in the ND2:SmoA1 transgenic mice, we crossed the ND2:SmoA1 mice with conditional (Nestin-Cre) N-*myc* knockout mice (11) to generate mice that possess persistently elevated Shh pathway activity in the cerebellum while lacking N-*myc* in the same region. These crosses produced four general groups of mice that we subsequently analyzed (Table 1). The number of mice that expressed ND2:SmoA1 and was null for N-*myc* in the cerebellum matched the number predicted by Mendelian inheritance, showing that this combination was not embryonic lethal.

The ND2:SmoA1 × N-*myc* conditional knockout mice were initially analyzed at 3 months of age. From birth onward, mice nullizygous for N-*myc* displayed moderate growth retardation and, by 3 weeks of age, began to exhibit tremors, an ataxic gait and raised tails, regardless of the presence or absence of the ND2:SmoA1 transgene. These phenotypes are also characteristic of the N-*myc* knockout mice (11). Forty-one mice were sacrificed at 3 months of age and it was noted that, compared with WT controls (Fig. 4*A*), nullizygous N-*myc* mice had significantly diminished cerebella in both the presence (Fig. 4*C*) and absence (Fig. 4*D*) of the ND2:SmoA1 transgene. Expression of the ND2:SmoA1 transgene was confirmed by immunofluorescent staining against the His tag present on the Smo protein encoded by the ND2:SmoA1 transgene. Staining with an anti-His antibody verified the expression of the ND2:SmoA1 transgene within granule cells of the N-*myc* null, ND2:SmoA1$^+$ (N-*myc*$^?$, SmoA1$^+$) cerebella (Fig. 5*A*) as was seen in N-*myc*$^{WT/WT}$, ND2:SmoA1$^+$ controls (Fig. 5*C*). Therefore, ND2:SmoA1 expression was not disrupted by the loss of N-*myc*, and expression occurs throughout the remaining GNP population.

Histologic examination revealed a strong reduction in cerebellar foliation in mice lacking N-*myc*, regardless of the presence (Fig. 4*G*) or absence (Fig. 4*H*) of the ND2:SmoA1 transgene. Note that the granular, molecular, and Purkinje cell layers are present. Additionally, the expression of Ki-67 and nestin was not observed in cerebella lacking N-*myc* (Fig. 3*D* and *H*), suggesting that N-*myc* may be required for maintaining a proliferative, precursor-like

DOI:10.1158/0008-5472.CAN-06-1621



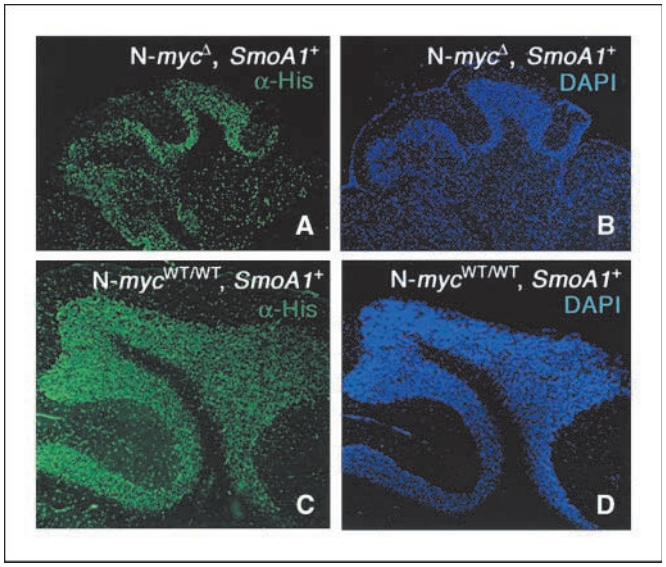


**Figure 5.** Loss of N-*myc* does not disrupt expression of the ND2:SmoA1 transgene in the granular layer of the cerebellum. *A,* immunofluorescent staining against the His tag on the ND2:SmoA1 transgene shows ND2:SmoA1 expression within the granule cells in an N-*myc*$^{?}$, SmoA1$^{+}$ cerebellum. *B,* a DAPI costain of the cerebellar section shown in (*A*), indicating the location of the granular layer. *C,* immunofluorescent staining against the His tag on the ND2:SmoA1 transgene, showing ND2:SmoA1 expression in an N-*myc*$^{WT/WT}$, SmoA1$^{+}$ control cerebellar section. *D,* a DAPI costain of the section shown in (*C*). Sections were taken at 3 months and shown at ×10 magnification.

population of cells during Shh-induced tumorigenesis. That constitutive activation of Smo fails to reverse the nullizygous N-*myc* overall brain and cerebellar-specific phenotypes suggests that N-*myc* is a critical downstream effector of Smo in the Shh signaling pathway. These findings also showed the requirement for N-*myc* in Shh-induced hyperplasia and in the persistent EGL observed in the majority of mice carrying the ND2:SmoA1 transgene.

**N-*myc* is required for tumorigenesis induced by deregulated Shh signaling.** Further analysis was carried out in mice at 6 months of age to examine the requirement for N-*myc* in ND2:SmoA1-driven medulloblastoma formation. Fifty-five mice from our study were sacrificed at 6 months. Mice nullizygous for N-*myc* and positive for the ND2:SmoA1 transgene phenotypically resembled the N-*myc* conditional knockout mice with significantly diminished cerebella (Fig. 4*C*). Histologic analysis at this time point revealed that mice lacking N-*myc* (Fig. 4*G* and *H*) have defects in cerebellar foliation compared with that of WT controls (Fig. 4*E*), with a reduction of the granular layer despite the presence of the ND2:SmoA1 transgene. No evidence of hyperproliferation or tumor formation was detected in mice lacking N-*myc* or in the WT controls (Table 1). Mice WT for N-*myc* and positive for the ND2:SmoA1 transgene developed hyperplasia and tumors (Fig. 4*B* and *F*) with an incidence similar to that seen in the study of the ND2:SmoA1 model (Table 1). These results indicate that N-*myc* is necessary for the hyperproliferation and tumor formation induced by the ND2:SmoA1 transgene. Furthermore, the hyperactivity of the Shh signaling pathway induced by the ND2:SmoA1 transgene is unable to compensate for the loss of N-*myc* in both normal GNP expansion as well as in hyperproliferation and tumor formation. Taken together, these findings provide *in vivo* evidence that N-*myc* acts downstream of Shh and Smo signaling during GNP proliferation and that N-*myc* is required for medulloblastoma genesis even in the presence of constitutively active signaling from the Shh pathway.

Although the loss of N-*myc* limits the expansion of the GNP population during normal cerebellar development, its loss does not ablate these cells entirely. GNPs are still specified and the granular layer does not fail to form. Thus, the cells thought to be the originators of tumor formation are still present within cerebella lacking N-*myc*. The phenotype of the N-*myc* null cerebellum was attributed previously to the inhibition of GNP proliferation. In addition, precocious differentiation of precursor cells in the cerebral cortex in the absence of N-*myc* was hypothesized to contribute to the failure of overall brain growth (11), indicating that N-*myc* may be functioning to maintain cells in a progenitor-like state. This role is consistent with the function of the Shh signaling pathway, which has been shown to prevent the terminal differentiation of GNPs (3, 4, 26), and whose deregulation might contribute to maintaining a subpopulation of GNPs in a progenitor-like state during tumorigenesis. The results of this study also suggest that other components of the Shh signaling pathway are unable or insufficient to activate the proliferative machinery of cell in the absence of N-*myc* despite the constitutive activation of the Smoothened signal beginning in early embryonic development, showing that N-*myc* plays a central role in Shh-mediated proliferation and tumorigenesis.

The requirement for N-*myc* during Shh-induced hyperplasia and tumorigenesis makes it an appealing target for therapeutic intervention in the treatment of medulloblastoma. Studies using GNP cultures have shown that the overexpression of N-*myc* can rescue the inhibition induced by treatment of these cultures with the Shh/Smo antagonist cyclopamine (21). Taken together with the results of our current study, these findings suggest that the prevention of overactive Shh signaling through the inhibition of N-*myc* activity may be beneficial. Our study shows that N-*myc* is a necessary downstream effector of Shh/Smo signals *in vitro* and *in vivo* and that N-*myc* may be an efficient target for the prevention of tumor growth because it may act as an integrator of multiple signaling pathways that act to drive GNP proliferation, in addition to being a key effector of the Shh signaling pathway. N-*myc* levels in GNPs are regulated in part by glycogen synthase kinase-3β phosphorylation, which targets N-*myc* for proteasome degradation (33). Therefore, antagonism of N-*myc* activity by phosphatidylinositol 3-kinase blockade or other targeted therapies could lead to a clinically relevant reduction in the pool of proliferating cells that progress to malignant tumors.

## Acknowledgments

Received 5/3/2006; revised 6/19/2006; accepted 6/23/2006.

**Grant support:** NIH grant CA112350-01, Children's Brain Tumor Foundation, and Damon Runyon Clinical Investigator Award (B.A. Hatton and J.M. Olson); NIH grant CA114400-01 (P.S. Knoepfler); Medical Foundation, Inc. and Sontag Foundation (A.M. Kenney); National Institute of Neurological Disorders and Stroke and James McDonnel Foundation (D.H. Rowitch); Spanish Ministry of Education and Science (I.M. de Alborán); and NIH grant CA20525 (R.N. Eisenman).

The costs of publication of this article were defrayed in part by the payment of page charges. This article must therefore be hereby marked *advertisement* in accordance with 18 U.S.C. Section 1734 solely to indicate this fact.

We thank Linda Cherepow in the Histopathology Shared Resource at Fred Hutchinson Cancer Research Center (Seattle, WA) for sectioning and H&E staining the transgenic mouse tissues, Jennifer Stoeck for assistance with transgenic animals, and Tina Xu for excellent technical assistance.

DOI:10.1158/0008-5472.CAN-06-1621



## References


1. Packer RJ, Cogen P, Vezina G, Rorke LB. Medulloblastoma: clinical and biologic aspects. Neuro-oncol 1999;1:232–50.
2. Rubin JB, Rowitch DH. Medulloblastoma: a problem of developmental biology. Cancer Cell 2002;2:7–8.
3. Dahmane N, Ruiz-i-Altaba A. Sonic hedgehog regulates the growth and patterning of the cerebellum. Development 1999;126:3089–100.
4. Wechsler-Reya RJ, Scott MP. Control of neuronal precursor proliferation in the cerebellum by Sonic hedgehog. Neuron 1999;22:103–14.
5. Wang VY, Zoghbi HY. Genetic regulation of cerebellar development. Nat Rev Neurosci 2001;2:484–91.
6. Corrales JD, Blaess S, Mahoney EM, Joyner AL. The level of sonic hedgehog signaling regulates the complexity of cerebellar foliation. Development 2006;133:1811–21.
7. Dahmane N, Sanchez P, Gitton Y, et al. The Sonic hedgehog-Gli pathway regulates dorsal brain growth and tumorigenesis. Development 2001;128:5201–12.
8. Murone M, Rosenthal A, de Sauvage FJ. Sonic hedgehog signaling by the patched-smoothened receptor complex. Curr Biol 1999;9:76–84.
9. Kenney AM, Cole MD, Rowitch DH. Nmyc upregulation by sonic hedgehog signaling promotes proliferation in developing cerebellar granule neuron precursors. Development 2003;130:15–28.
10. Duman-Scheel M, Weng L, Xin S, Du W. Hedgehog regulates cell growth and proliferation by inducing cyclin d and cyclin E. Nature 2002;417:299–304.
11. Knoepfler PS, Cheng PF, Eisenman RN. N-*myc* is essential during neurogenesis for the rapid expansion of progenitor cell populations and the inhibition of neuronal differentiation. Genes Dev 2002;16:2699–712.
12. Pomeroy SL, Tamayo P, Gaasenbeek M, et al. Prediction of central nervous system embryonal tumour outcome based on gene expression. Nature 2002;415:436–42.
13. Vorechovsky I, Tingby O, Hartman M, et al. Somatic mutations in the human homologue of *Drosophila* patched in primitive neuroectodermal tumours. Oncogene 1997;15:361–6.
14. Taylor MD, Liu L, Raffel C, et al. Mutations in SUFU predispose to medulloblastoma. Nat Genet 2002;31:306–10.
15. Berman DM, Karhadkar SS, Hallahan AR, et al. Medulloblastoma growth inhibition by hedgehog pathway blockade. Science 2002;297:1559–61.
16. Hallahan AR, Pritchard JI, Hansen S, et al. The SmoA1 mouse model reveals that notch signaling is critical for the growth and survival of sonic hedgehog-induced medulloblastomas. Cancer Res 2004;64:7794–800.
17. Marino S. Medulloblastoma: developmental mechanisms out of control. Trends Mol Med 2005;11:17–22.
18. Adhikary S, Eilers M. Transcriptional regulation and transformation by Myc proteins. Nat Rev Mol Cell Biol 2005;6:635–45.
19. Grandori C, Cowley SM, James LP, Eisenman RN. The Myc/Max/Mad network and the transcriptional control of cell behavior. Annu Rev Cell Dev Biol 2000;16:653–99.
20. Fults D, Pedone C, Dai C, Holland EC. MYC expression promotes the proliferation of neural progenitor cells in culture and *in vivo*. Neoplasia 2002;4:32–9.
21. Oliver TG, Grasfeder LL, Carroll AL, et al. Transcriptional profiling of the Sonic hedgehog response: a critical role for N-*myc* in proliferation of neuronal precursors. Proc Natl Acad Sci U S A 2003;100:7331–6.
22. Xie J, Murone M, Luoh SM, et al. Activating Smoothened mutations in sporadic basal-cell carcinoma. Nature 1998;391:90–2.
23. Reifenberger J, Wolter M, Weber RG, et al. Missense mutations in SMOH in sporadic basal cell carcinomas of the skin and primitive neuroectodermal tumors of the central nervous system. Cancer Res 1998;58:1798–803.
24. Taipale J, Beachy PA. The hedgehog and Wnt signalling pathways in cancer. Nature 2001;411:349–54.
25. Taipale J, Chen JK, Cooper MK, et al. Effects of oncogenic mutations in Smoothened and Patched can be reversed by cyclopamine. Nature 2000;406:1005–9.
26. Kenney AM, Rowitch DH. Sonic hedgehog promotes $G_1$ cyclin expression and sustained cell cycle progression in mammalian neuronal precursors. Mol Cell Biol 2000;20:9055–67.
27. Bartz SR, Vodicka MA. Production of high-titer human immunodeficiency virus type 1 pseudotyped with vesicular stomatitis virus glycoprotein. Methods 1997;12:337–42.
28. de Alboran IM, O'Hagan RC, Gartner F, et al. Analysis of C-MYC function in normal cells via conditional gene-targeted mutation. Immunity 2001;14:45–55.
29. Tronche F, Kellendonk C, Kretz O, et al. Disruption of the glucocorticoid receptor gene in the nervous system results in reduced anxiety. Nat Genet 1999;23:99–103.
30. Knoepfler PS, Zhang XY, Cheng PF, Gafken PR, McMahon SB, Eisenman RN. Myc influences global chromatin structure. EMBO J. Epub ahead of print 2006 May 25; doi:10.1038/sj.emboj.7601152.
31. Wallace VA. Purkinje-cell-derived Sonic hedgehog regulates granule neuron precursor cell proliferation in the developing mouse cerebellum. Curr Biol 1999;9:445–8.
32. Zimmerman KA, Yancopoulos GD, Collum RG, et al. Differential expression of myc family genes during murine development. Nature 1986;319:780–3.
33. Kenney AM, Widlund HR, Rowitch DH. Hedgehog and PI-3 kinase signaling converge on Nmyc1 to promote cell cycle progression in cerebellar neuronal precursors. Development 2004;131:217–28.